PB83-140731

ENAMAP-1A Long Term Air Pollution Model Refinement of Transformation and Deposition Mechanisms

SRI International
Menlo Park, CA

Prepared for

Environmental Sciences Research Lab.
Research Triangle Park, NC

1982

U.S. Department of Commerce
National Technical Information Service
NTIS

PB83-140731
EPA-600/D-82-351
PUBLISHED PAPER

ENAMAP-1 LONG TERM AIR POLLUTION MODEL: REFINEMENT OF TRANSFORMATION AND DEPOSITION MECHANISMS

Roy M. Endlich, Chandrakant M. Bhumralkar, Richard Brodzinsky, Kenneth C. Nitz, and Bruce K. Cantrell
SRI International

and

Peter M. Mayerhofer
Meteorology Applications

and

Terry L. Clark
U.S. Environmental Protection Agency

Atmospheric Science Center, SRI International
333 Ravenswood, Menlo Park, California 94025

REPRODUCED BY
NATIONAL TECHNICAL
INFORMATION SERVICE
U.S. DEPARTMENT OF COMMERCE
SPRINGFIELD, VA 22161

TECHNICAL REPORT DATA (Please read Instructions on the reverse before complet		
1. REPORT NO. EPA-600/D-82-351	2. Published Paper	3. PB83-140731
4. TITLE AND SUBTITLE ENAMAP-1A LONG TERM AIR POLLUTION MODEL : REFINEMENT OF TRANSFORMATION AND DEPOSITION MECHANISMS		5. REPORT DATE 1982
		6. PERFORMING ORGANIZATION CODE
7. AUTHOR(S) R.M. Endlich, C.M. Bhumralkar, R. Brodzinsky, K. Nitz, B.K. Cantrell, P.M. Mayerhofer, and T.L. Clark		8. PERFORMING ORGANIZATION REPORT NO.
9. PERFORMING ORGANIZATION NAME AND ADDRESS SRI, International 333 Ravenswood Avenue Menlo Park, CA 94025		10. PROGRAM ELEMENT NO. CCVN1A/01-0511 (FY-82)
		11. CONTRACT/GRANT NO. EPA 68-02-3424
12. SPONSORING AGENCY NAME AND ADDRESS Environmental Sciences Research Laboratory--RTP,NC Office of Research and Development U.S. Environmental Protection Agency Research Triangle Park, NC 27711		13. TYPE OF REPORT AND PERIOD COVERED
		14. SPONSORING AGENCY CODE EPA/600/09
15. SUPPLEMENTARY NOTES		

16. ABSTRACT

This paper is concerned with the long-range transport of air pollution over eastern North America. Using standard weather reports and several SO_x emission data inventories, the ENAMAP model computes the airborne concentrations of SO_2 and $SO_4^=$ and their deposition on the earth's surface. The newest version of the model (ENAMAP-1B) includes the influences of smoothed terrain on the winds and divides the atmospheric boundary layer into three parts. This treatment allows pollution emissions to be divided among layers. Vertical mixing is controlled by diffusion coefficients computed from wind shear, stability, and the mixing depth. Recent published values are used for transformation and wet and dry deposition rates; however, there are still major uncertainties in these values.

The model has been used to compute monthly average values of concentration and deposition for January and August 1977. Comparisons with air quality measurements show that calculated SO_2 concentrations are reasonably accurate, but $SO_4^=$ concentrations are generally too high. Further tuning of the model is required to optimize its performance. A version of the model applicable to NO_x emissions is currently being tested.

17. KEY WORDS AND DOCUMENT ANALYSIS		
a. DESCRIPTORS	b. IDENTIFIERS/OPEN ENDED TERMS	c. COSATI Field/Group
18. DISTRIBUTION STATEMENT RELEASE TO THE PUBLIC	19. SECURITY CLASS (This Report) UNCLASSIFIED	21. NO. OF PAGES 20
	20. SECURITY CLASS (This page) UNCLASSIFIED	22. PRICE

EPA Form 2220-1 (9-73)

82-10.3

ENAMAP-1A LONG TERM AIR POLLUTION MODEL, R.M. Endlich, C. Bhumralkar, R. Brodzinsky, K. Nitz, and B. Cantrell, SRI Intn'l., Menlo Park, CA 94025; P. Mayerhofer, MAI, Menlo Park, CA 94025; and T. Clark, EPA, Research Triangle Park, NC

This paper is concerned with the long-range transport of air pollution over eastern North America. Using standard weather reports and several SO_x emissions data inventories, the ENAMAP model computes the airborne concentrations of SO_2 and $SO_4^=$ and their deposition on the earth's surface. The newest version of the model (ENAMAP-1B) includes the influences of smoothed terrain on the winds, and divides the atmospheric boundary layer into three parts. This treatment allows pollution emissions to be divided among the layers. Vertical mixing is controlled by diffusion coefficients computed from wind shear, stability and knowledge of the mixing depth. Recent published values are used for transformation, and wet and dry deposition rates; however, there are still major uncertainties in these values.

The model has been used to compute monthly average values of concentration and deposition for January and August 1977. Comparisons with air quality measurements show that calculated SO_2 concentrations are reasonably accurate, but $SO_4^=$ concentrations are generally too high. Further tuning of the model is required to optimize its performance. A version of the model applicable to NO_x emissions is currently being tested.

Introduction

Under sponsorship of EPA, SRI[1,2,3] has developed a numerical model that simulates the transport of air pollution over long distances. The model computes the airborne concentration of pollution and its deposition by dry and wet processes on the earth's surface. Analyses are made of radiosonde measurements of wind and temperature in order to obtain representative wind and stability fields, which vary in space and time. By tracking pollution puffs, the model is able to identify source-receptor relationships, i.e., how much of the pollution in a region was emitted locally, and how much originated in other specified areas. The complicated meteorological and chemical processes of air pollution are represented by algorithms that provide practical and efficient computations.

Description of the Model

The functional parts of ENAMAP are shown in Figure 1. The model domain covers the eastern United States and southeastern Canada (Figure 2). This domain is represented by a 70 km grid mesh. The annual emissions of SO_2 and $SO_4^=$ (based on data from the SURE and NEDS inventories and from Environment Canada) are shown in Figure 3; the major source areas are clearly indicated. (Isolines in Figure 3 are drawn at intervals of 4, 16, 64, 256, etc.) The largest value of the SO_2 emissions (on the Ohio-Pennsylvania border) is 150.7 tons km^{-2} and the corresponding $SO_4^=$ emissions are 4.9 tons km^{-2}. In the model, SO_2 and $SO_4^=$ are emitted from 41 separate regions and the impact is calculated for the same receptor areas. Transport winds are computed at the grid points from radiosonde reports at 12-hour intervals and from surface observations at 3-hour intervals. The boundary layer is divided into three parts using terrain-following coordinates as shown in Figure 4. The boundary layer top is taken at a climatological value of height except over a few points where the smoothed terrain is higher than approximately 1 km; at these points the boundary layer is taken to be 500m thick. The top of the first layer is at approximately 200m (for locations near sea level), and the top of the second layer is at approximately 700m. The winds are adjusted to be non-divergent within these layers before being used in the transport computations. The adjustment causes the winds to speed up over higher terrain and to pass around major obstacles.

Emissions are introduced into the layers in a different manner in the daytime than at night. In the daytime we assume that rapid mixing occurs throughout the boundary layer; therefore emissions are partitioned initially to give equal concentrations in the layers. At night, mixing is inhibited by thermal stability. For point sources of either SO_2 or NO_x the typical plume rise is several hundred meters; therefore point sources initially enter layer 2 (see Figure 5). The 1977 SO_2 emissions were predominately (90 percent) from point sources; therefore at night all SO_2 emissions are initially placed in layer 2. NO_x pollutants were divided approximately evenly between point and area sources. Point source NO_x is placed initially in layer 2 for the reasons given above. On the other hand, most NO_x area emissions come from vehicles; therefore all NO_x area emissions are placed initially in layer 1 (Figure 5).

Vertical mixing in ENAMAP is based on a finite-difference form of the expression

$$\partial C/\partial t = \partial/\partial z \left[D_z \, (\partial C/\partial z) \right] .$$

The vertical diffusion coefficients D_z are computed as a function of wind shear, stability, and the height of the mixing depth. The values used in the computation reported in this paper fall in the range from 1 to 10 $m^2 s^{-1}$.

The chemical processes simulated in ENAMAP-1B are summarized in Figure 6. The transformation of SO_2 to $SO_4^=$ depends on solar insolation and therefore varies with season and latitude[4]. The dry deposition velocity is based on the surface characteristics (water or land-use type) as well as on thermal stability[5]. The stability class is computed from wind speed, cloud cover, and time of day[6]. The dry deposition velocities vary over a wide range[3]. For SO_2 at night a relatively low dry deposition rate of 0.07 cm s^{-1} is used everywhere to account for low adsorption by plant surfaces. Wet deposition rates used in ENAMAP-1B are the largest for summertime (convective) rain[7]. In our earlier work we used larger wet deposition rates, especially in winter. All these chemical rates are somewhat uncertain because they are based to a large extent on laboratory measurements.

At present we are testing a form of ENAMAP-1B that applies to NO_x emissions. The complicated chemistry of nitrogen compounds is represented in a simplified way using the five species NO, NO_2, PAN, HNO_3, and NO_3^-. Appropriate reaction rates, equilibrium constants, and deposition velocities are prescribed insofar as they are known. Results from this model will be available in the near future.

Results

The model was run for the months of January and August 1977, and monthly average values of wet and dry deposition and airborne concentration were computed for SO_2 and $SO_4^=$. Maps showing typical results for January 1977 are given in Figures 7, 8, 9, and 10. The patterns of concentration and deposition naturally are closely related to the emission sources, and the SO_2 and $SO_4^=$ concentrations have largest values downwind from the Ohio River valley. The calculated and observed concentrations of SO_2 are in general agreement; however, there are significant local differences. The calculated $SO_4^=$ concentrations generally are somewhat higher than the observed values. The wet deposition patterns (Figure 9) reflect the rainfall patterns for the month. No wet deposition is indicated for Canada because the Canadian precipitation data that were used do not include snowfall, which is of course predominant in January. The dry deposition amounts in January (Figure 10) are much larger and more widespread than the wet deposition amounts. Similar patterns were computed for August 1977.

The model also gives source-receptor relationships as illustrated in Tables I and II. The columns of Table I show the contribution of each individual area to the total sulfur deposition (SO_2 and $SO_4^=$ combined) within that area. For example, column 23 (for New York) shows that 4.1 KTON S originated in Michigan (row 14), 2.7 KTON originated in New York itself, and 4.5 KTON originated in

Ohio (row 26). The total deposition in New York in January 1977 was 27.7 KTON S. Table II is a similar tabulation for SO_2 airborne concentration. The model also gives all of these entries as percentages of totals received. From this information, the influence of pollution sources in one area on the surrounding areas can be determined.

The verification of computations of this type is a difficult task for several reasons. These include problems in measuring emissions, concentrations, and depositions, and the need to avoid local, unrepresentative effects. For the January and August 1977 computations the principal validation data are SO_2 and $SO_4^=$ concentrations from the SURE and SAROAD inventories. These air quality data were averaged over 160 by 160 km areas to smooth the effects of local values. Scatter diagrams showing typical results (actually from earlier runs of the model) are shown in Figure 11 for SO_2 and in Figure 12 for $SO_4^=$. There is a great deal of scatter and the $SO_4^=$ results also show a bias in the calculations toward too-high values particularly for the August data.

We are planning to optimize the model by monitoring its performance while using different values of those parameters that are relatively uncertain.

Summary

Experience with ENAMAP-1B shows that it has the following advantages:

1) The puff-tracking methodology identifies the source-receptor relationships among different areas, i.e., the amount of pollution in an area that originates in all areas of the model domain.

2) Emissions can be introduced in layers in an appropriate manner.

3) The model is sufficiently economical that computations can be made for long time periods (such as a month).

4) For SO_x pollutants the accuracy of the results is reasonably good. Improved results are expected by tuning the model with available observations.

The model is subject to the following limitations:

1) The results are dependent on rates for several chemical processes; these rates are rather uncertain and are under continuing investigation by various groups.

2) The pollution patterns from single sources of emissions are not identified.

3) It is not possible to include nonlinear chemistry in this type of model, as chemical processes due to mixing of puffs are not simulated.

A complete report concerning the model, including its application to NO_x emissions, is currently being prepared.

Achnowledgment

The SRI research has been carried out under EPA Contract 68-02-3424.

References

1. C. M. Bhumralkar, R. L. Mancuso, D. E. Wolf, R. H. Thuillier, K. C. Nitz, and W. B. Johnson, "Adaptation and application of a long-term air pollution model ENAMAP-1 to eastern North America," Final Report, Contract 68-02-2959, SRI International, Menlo Park, California (1980a).

2. C. M. Bhumralkar, R. L. Mancuso, D. E. Wolf, K. C. Nitz, and W. B. Johnson, "Adaptation and application of the ENAMAP-1 model to eastern North America--Phase II," Final Report, Contract 68-02-2959, SRI International, Menlo Park, California (1980b).

3. P. M. Mayerhofer, R. M. Endlich, B. K. Cantrell, R. Brodzinsky, and C. M. Bhumralkar, "ENAMAP-1A long term SO_2 and sulfate air pollution model: refinement of transformation and deposition mechanisms," Final Report, Contract 68-02-3424, SRI International, Menlo Park, California (1981).

4. A. P. Altshuller, "Model predictions of the rates of homogeneous oxidation of sulfur dioxide to sulfate in the troposphere," Atmos. Environ. 13:1653.

5. C. M. Sheih, M. L. Wesely, and B. B. Hicks, "Estimated dry deposition velocities of sulfur over the eastern United States and surrounding regions," Atmos. Environ. 13:1361.

6. D. B. Turner, "Workbook of atmospheric dispersion estimates," PHS Publication No. 999-AP-26. U.S. Department of Health, Education, and Welfare, NAPCA, Cincinnati, Ohio (1969).

7. B. C. Scott, "Parameterization of sulfate removal by precipitation," J. Appl. Met. 17:1375.

Table I

EXAMPLE OF COMPUTED SULFUR DEPOSITION DUE TO
INTERREGIONAL EXCHANGES OF AIRBORNE SULFUR IN JANUARY 1977
(Units are KTON Sulfur)

EMITTER REGION	TOTAL CONTRIBUTIONS TO S DEPOSITIONS WITHIN RECEPTOR REGIONS 16	17	18	19	20	21	22	23	24	25	26	27	28	29	30
1 ALABAMA	2.1	.0	0.	0.	.0	.0	0.	.0	2.2	0.	.0	0.	.0	.0	2.0
2 ARKANSAS	.3	.1	0.	.0	.0	.0	0.	.0	.1	0.	.0	.0	.0	.0	.1
3 COLORADO	0.	0.	0.	0.	0.	0.	0.	0.	0.	0.	0.	0.	0.	0.	0.
4 DEL/MD/DC	0.	0.	0.	0.	.0	.2	0.	.1	.1	0.	.0	0.	.2	.0	.0
5 FLORIDA	.0	0.	0.	0.	0.	0.	0.	0.	.0	0.	0.	0.	0.	0.	.1
6 GEORGIA	.2	0.	0.	0.	0.	.0	0.	0.	1.9	0.	0.	0.	0.	0.	2.1
7 ILLINOIS	.8	2.1	0.	0.	.8	.4	0.	2.1	1.8	0.	4.2	.0	2.1	.7	.9
8 INDIANA	.0	.3	0.	0.	.8	.7	0.	2.7	1.7	0.	7.9	0.	3.3	.9	.7
9 IOWA	.1	.4	0.	.0	.1	.0	0.	.3	.1	0.	.5	.1	.2	.1	.0
10 KANSAS	.0	.2	0.	.0	.0	.0	.0	.0	.0	0.	.0	.1	.0	.0	.0
11 KENTUCKY	.1	.0	0.	0.	.3	.4	0.	.8	3.3	0.	2.9	0.	2.0	.5	1.0
12 LOUISIANA	1.0	.0	0.	0.	.0	.0	0.	.0	.2	0.	.0	.0	.0	.0	.2
13 MAINE	0.	0.	0.	0.	.2	.0	0.	.0	0.	0.	0.	0.	.0	.1	0.
14 MICHIGAN	0.	.0	0.	0.	1.6	.5	0.	4.1	.0	0.	2.5	0.	2.2	.9	.0
15 MINNESOTA	.1	.1	0.	.0	.1	.0	0.	.3	.0	.0	.5	.0	.3	.1	.0
16 MISS.	.9	.0	0.	0.	.0	.0	0.	.0	.1	0.	0.	.0	.0	.0	.1
17 MISSOURI	1.6	4.9	0.	.0	.3	.2	0.	.8	.7	0.	1.4	.5	1.0	.3	.3
18 MONTANA	0.	0.	0.	0.	0.	0.	0.	0.	0.	0.	0.	0.	0.	0.	0.
19 NEBRASKA	.0	.0	.0	.0	.0	.0	.0	.0	.0	.0	.0	.0	.0	.0	.0
20 NH/VT	0.	0.	0.	0.	.3	.0	0.	.2	0.	0.	0.	0.	.0	.5	0.
21 NEW JERSEY	0.	0.	0.	0.	.0	.6	0.	.1	.0	0.	0.	0.	.2	.2	0.
22 NEW MEXICO	0.	0.	0.	0.	0.	0.	0.	0.	0.	0.	0.	0.	0.	0.	0.
23 NEW YORK	0.	0.	0.	0.	.8	1.0	0.	2.7	.0	0.	.0	0.	.8	1.6	0.
24 N CAROLINA	0.	0.	0.	0.	0.	.0	0.	.0	3.5	0.	.0	0.	.0	.0	1.1
25 N DAKOTA	.0	.0	.0	.0	.0	.0	.0	.0	.0	.2	.0	.0	.0	.0	.0
26 OHIO	0.	0.	0.	0.	1.0	1.2	0.	4.5	.7	0.	5.4	0.	7.6	1.5	.0
27 OKLAHOMA	.2	.2	0.	.0	.0	.0	.0	.0	.0	0.	.0	.5	.0	.0	.0
28 PENN.	0.	0.	0.	0.	.7	1.8	0.	2.9	.1	0.	.5	0.	6.3	1.7	0.
29 RI/MA/CT	0.	0.	0.	0.	.0	.0	0.	.1	0.	0.	0.	0.	.0	.4	0.
30 S CAROLINA	0.	0.	0.	0.	0.	.0	0.	0.	1.0	0.	0.	0.	0.	0.	1.4
31 S DAKOTA	.0	.0	.0	.0	.0	.0	.0	.0	.0	.0	.0	.0	.0	.0	.0
32 TENNESSEE	.9	.1	0.	0.	.0	.1	0.	.1	2.8	0.	.2	0.	.2	.1	1.6
33 TEXAS	.5	.1	0.	.0	.0	.0	.0	.0	.1	0.	.0	.6	.0	.0	.1
34 VIRGINIA	0.	0.	0.	0.	.0	.1	0.	.0	2.1	0.	.0	0.	.1	.0	.2
35 W VIRGINIA	0.	0.	0.	0.	.4	1.2	0.	2.2	.7	0.	1.4	0.	6.9	1.4	.0
36 WISCONSIN	.0	.1	0.	0.	.3	.1	0.	.8	.1	0.	1.0	.0	.5	.2	.0
37 MANITOBA	.0	.0	0.	.0	.0	.0	0.	.0	.0	.0	.0	.0	.0	.0	.0
38 N BRUNS	0.	0.	0.	0.	.0	0.	0.	.0	0.	0.	0.	0.	0.	.0	0.
39 ONTARIO	0.	.0	0.	0.	1.1	.1	0.	2.4	.0	.0	.2	0.	.4	.5	0.
40 QUEBEC	0.	0.	0.	0.	.6	.0	0.	.4	0.	0.	.0	0.	.0	.1	0.
41 NEWFOUND	0.	0.	0.	0.	0.	0.	0.	0.	0.	0.	0.	0.	0.	0.	0.
TOTAL (KTON S)	8.8	8.7	.0	.1	9.5	9.0	.0	27.7	23.5	.2	28.7	1.9	34.5	11.9	12.0

Table II

EXAMPLE OF COMPUTED SO_2 CONCENTRATION DUE TO
INTERREGIONAL EXCHANGES OF AIRBORNE SULFUR IN JANUARY 1977
(Units are KTON Sulfur)

EMITTER REGION	TOTAL CONTRIBUTIONS TO SO2 CONCENTRATIONS WITHIN RECEPTOR REGIONS 16	17	18	19	20	21	22	23	24	25	26	27	28	29	30
1 ALABAMA	2.1	.0	0.	0.	.0	.1	0.	.0	2.1	0.	.0	0.	.0	.0	3.4
2 ARKANSAS	.3	.1	0.	.0	.0	.0	0.	.0	.1	0.	.0	.0	.0	.0	.1
3 COLORADO	0.	0.	0.	0.	0.	0.	0.	0.	0.	0.	0.	0.	0.	0.	0.
4 DEL/MD/DC	0.	0.	0.	0.	.0	1.4	0.	.1	.1	0.	.0	0.	.4	.2	.0
5 FLORIDA	.0	0.	0.	0.	0.	0.	0.	0.	.0	0.	0.	0.	0.	0.	.1
6 GEORGIA	.1	0.	0.	0.	0.	.0	0.	0.	1.9	0.	0.	0.	0.	0.	4.1
7 ILLINOIS	.7	2.3	0.	0.	1.7	2.1	0.	2.1	1.6	0.	5.6	.0	2.7	1.9	1.3
8 INDIANA	.0	.3	0.	0.	2.2	3.9	0.	3.0	1.7	0.	12.8	0.	4.9	3.0	1.1
9 IOWA	.0	.4	0.	.0	.2	.2	0.	.2	.1	0.	.5	.1	.2	.1	.1
10 KANSAS	.0	.2	0.	.0	.0	.0	.0	.0	.0	0.	.0	.1	.0	.0	.0
11 KENTUCKY	.1	.0	0.	0.	.8	3.0	0.	1.0	3.8	0.	5.3	0.	2.9	1.8	1.7
12 LOUISIANA	1.2	.0	0.	0.	.0	.0	0.	.0	.1	0.	.0	.0	.0	.0	.2
13 MAINE	0.	0.	0.	0.	.8	.0	0.	.0	0.	0.	0.	0.	.0	.4	0.
14 MICHIGAN	0.	.0	0.	0.	4.1	2.4	0.	5.5	.0	0.	5.2	0.	4.0	2.8	.0
15 MINNESOTA	.1	.1	0.	.0	.3	.1	0.	.3	.0	.0	.5	.0	.2	.2	.0
16 MISS.	1.2	.0	0.	0.	.0	.0	0.	.0	.1	0.	0.	.0	.0	.0	.2
17 MISSOURI	1.6	7.1	0.	.0	.5	.9	0.	.6	.6	0.	1.7	.4	1.1	.6	.4
18 MONTANA	0.	0.	0.	0.	0.	0.	0.	0.	0.	0.	0.	0.	0.	0.	0.
19 NEBRASKA	.0	.1	.0	.1	.0	.0	.0	.0	.0	.0	.0	.0	.0	.0	.0
20 NH/VT	0.	0.	0.	0.	1.7	.2	0.	.2	0.	0.	0.	0.	.0	3.0	0.
21 NEW JERSEY	0.	0.	0.	0.	.1	6.7	0.	.2	.0	0.	0.	0.	.3	.8	0.
22 NEW MEXICO	0.	0.	0.	0.	0.	0.	0.	0.	0.	0.	0.	0.	0.	0.	0.
23 NEW YORK	0.	0.	0.	0.	3.0	8.2	0.	5.6	.0	0.	.0	0.	1.2	9.2	0.
24 N CAROLINA	0.	0.	0.	0.	0.	.0	0.	.0	5.3	0.	.0	0.	.0	.0	2.6
25 N DAKOTA	.0	.0	.0	.0	.0	.0	.0	.0	.0	.2	.0	.0	.0	.0	.0
26 OHIO	0.	0.	0.	0.	3.1	8.5	0.	5.7	.8	0.	12.2	0.	14.6	5.6	.0
27 OKLAHOMA	.1	.2	0.	.0	.0	.0	.0	.0	.0	0.	.0	.6	.0	.0	.0
28 PENN.	0.	0.	0.	0.	1.9	14.9	0.	4.3	.1	0.	.9	0.	16.3	6.5	0.
29 RI/MA/CT	0.	0.	0.	0.	.1	.2	0.	.1	0.	0.	0.	0.	.0	2.5	0.
30 S CAROLINA	0.	0.	0.	0.	0.	.0	0.	0.	1.1	0.	0.	0.	0.	0.	3.8
31 S DAKOTA	.0	.0	.0	.0	.0	.0	.0	.0	.0	.0	.0	.0	.0	.0	.0
32 TENNESSEE	1.2	.1	0.	0.	.1	.6	0.	.1	3.2	0.	.2	0.	.3	.3	3.1
33 TEXAS	.3	.0	0.	.0	.0	.0	.2	.0	.1	0.	.0	.6	.0	.0	.1
34 VIRGINIA	0.	0.	0.	0.	.0	.7	0.	.0	3.1	0.	.0	0.	.1	.1	.3
35 W VIRGINIA	0.	0.	0.	0.	1.4	8.9	0.	2.8	.8	0.	3.1	0.	14.0	5.1	.0
36 WISCONSIN	.0	.1	0.	0.	.7	.6	0.	.8	.0	0.	1.3	.0	.7	.5	.0
37 MANITOBA	.0	.0	0.	.0	.0	.0	0.	.0	.0	.0	.0	.0	.0	.0	.0
38 N BRUNS	0.	0.	0.	0.	.0	0.	0.	.0	0.	0.	0.	0.	0.	.0	0.
39 ONTARIO	0.	.0	0.	0.	3.4	.8	0.	3.7	.0	.0	.4	0.	.8	1.9	0.
40 QUEBEC	0.	0.	0.	0.	2.5	.1	0.	.5	0.	0.	.0	0.	.0	.4	0.
41 NEWFOUND	0.	0.	0.	0.	0.	0.	0.	0.	0.	0.	0.	0.	0.	0.	0.
TOTAL SO2 UG/M3	9.2	11.2	.0	.2	28.6	64.6	.2	37.1	26.7	.3	49.7	1.8	65.0	47.2	22.6

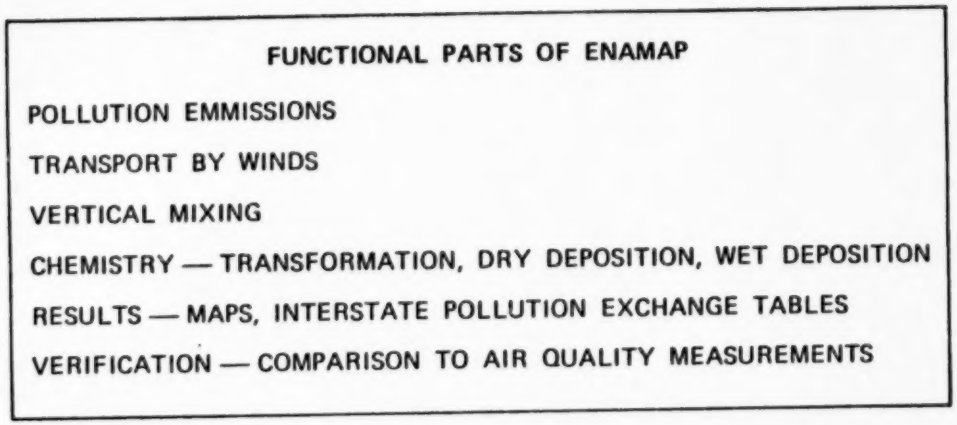
FUNCTIONAL PARTS OF ENAMAP
POLLUTION EMMISSIONS
TRANSPORT BY WINDS
VERTICAL MIXING
CHEMISTRY — TRANSFORMATION, DRY DEPOSITION, WET DEPOSITION
RESULTS — MAPS, INTERSTATE POLLUTION EXCHANGE TABLES
VERIFICATION — COMPARISON TO AIR QUALITY MEASUREMENTS

FIGURE 1 FUNCTIONAL PARTS OF THE ENAMAP MODEL.

FIGURE 2 EASTERN NORTH AMERICAN MODEL DOMAIN.

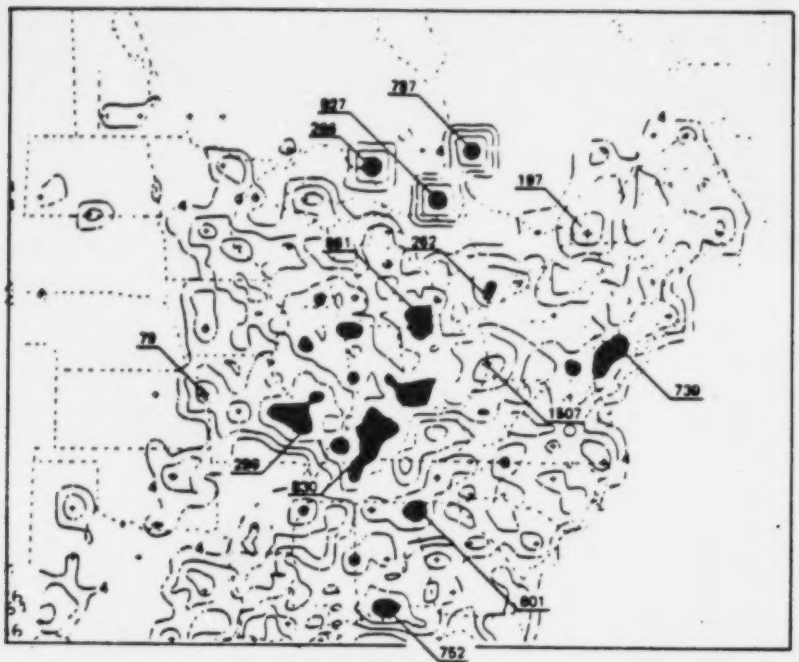

(a) SO_2

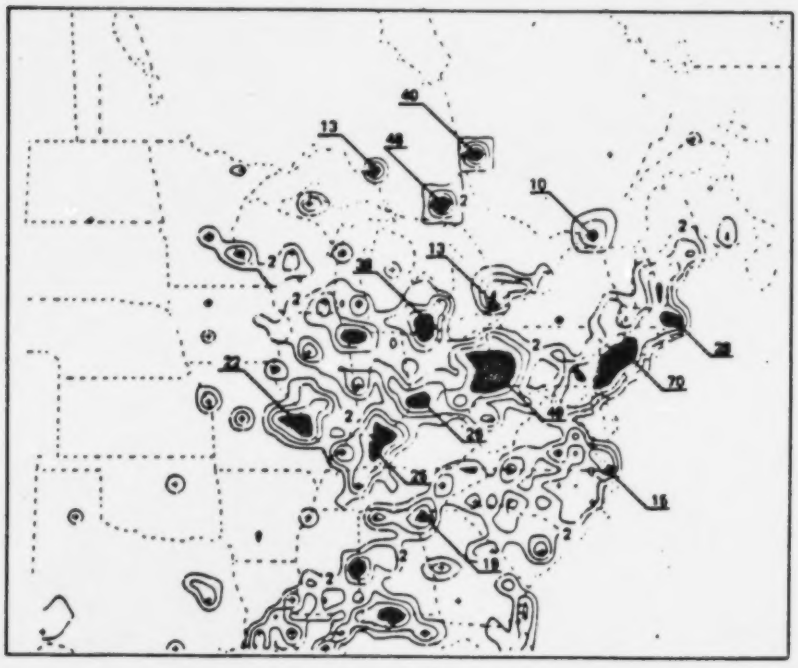

(b) $SO_4^=$

FIGURE 3 ANNUAL SO_2 AND $SO_4^=$ EMISSIONS FOR 1977 (10^{-1} ton km^{-2}).

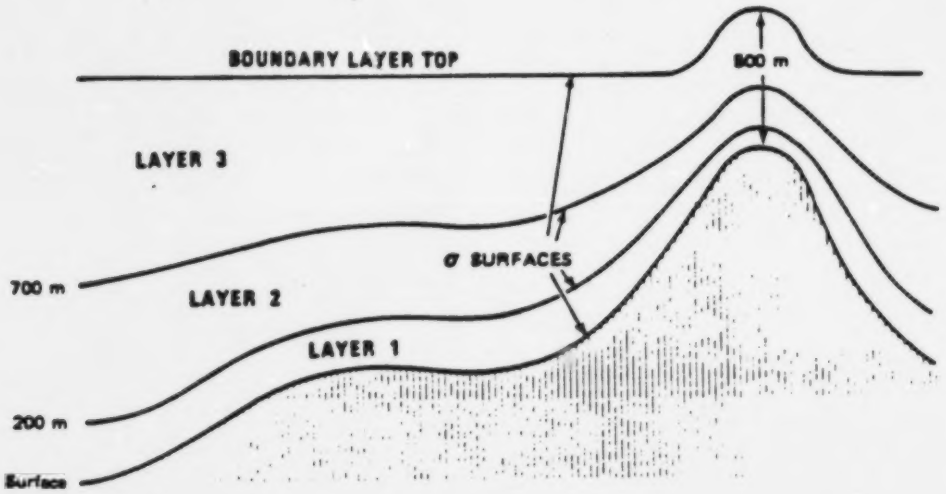

FIGURE 4 DIVISION OF THE BOUNDARY LAYER INTO THREE PARTS USING TERRAIN FOLLOWING COORDINATES.

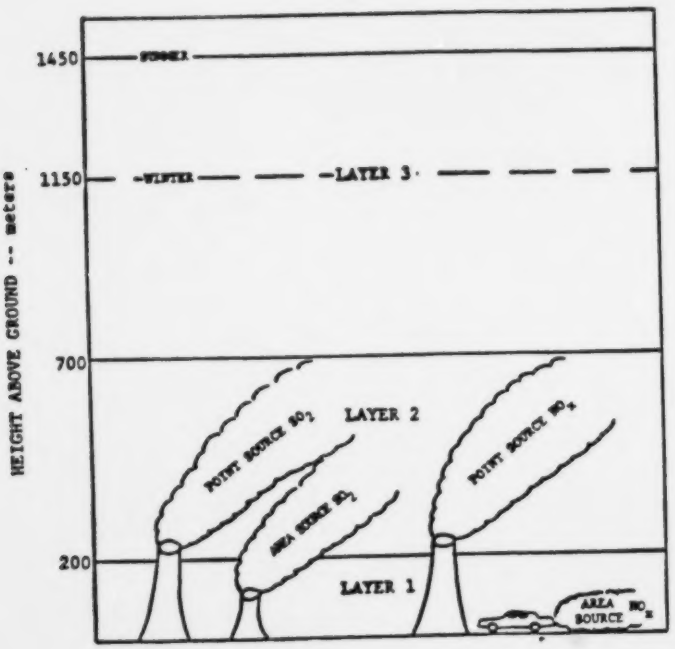

FIGURE 5 NIGHTTIME DISTRIBUTION OF EMISSIONS IN THE LAYERS OF ENAMAP-1B.

CHEMICAL PROCESSES FOR SULFUR COMPOUNDS

TRANSFORMATION OF SO_2 TO $SO_4^=$

DEPENDS ON SOLAR INSOLATION. VARIES FROM 0.01 h^{-1} (1% h^{-1}) IN WINTER TO 0.04 h^{-1} IN SUMMER.

WET DEPOSITION RATE

SO_2: DEPENDS ON RAINFALL TYPE AND RATE. FOR 5 mm h^{-1} OF RAIN, VARIES FROM 0.03 h^{-1} (WINTER) TO 0.17 h^{-1} (SUMMER).

$SO_4^=$: SIMILAR TO SO_2. FOR 5 mm h^{-1} OF RAIN, VARIES FROM 0.06 h^{-1} (WINTER) TO 0.43 h^{-1} (SUMMER).

DRY DEPOSITION VELOCITY

SO_2: DEPENDS ON LAND CHARACTERISTICS AND VEGETATION, STABILITY, SEASON AND TIME OF DAY. VALUES VARY FROM 0.05 cm s^{-1} TO 0.85 cm s^{-1}.

$SO_4^=$: SIMILAR TO SO_2 EXCEPT NO DEPENDENCE ON TIME OF DAY. VALUES VARY FROM 0.25 cm s^{-1} TO 0.95 cm s^{-1}.

FIGURE 6 CHEMICAL PROCESSES FOR SULFUR COMPOUNDS INCLUDED IN THE MODEL.

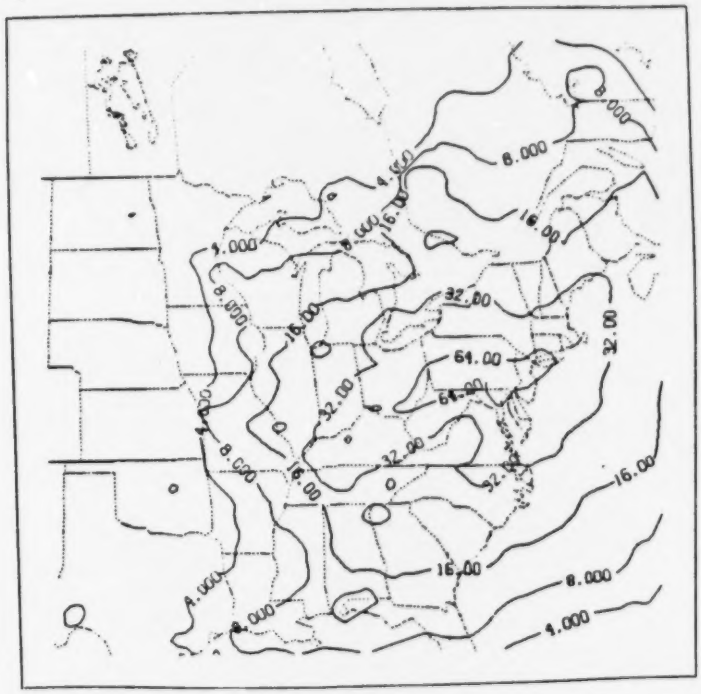

(Upper)

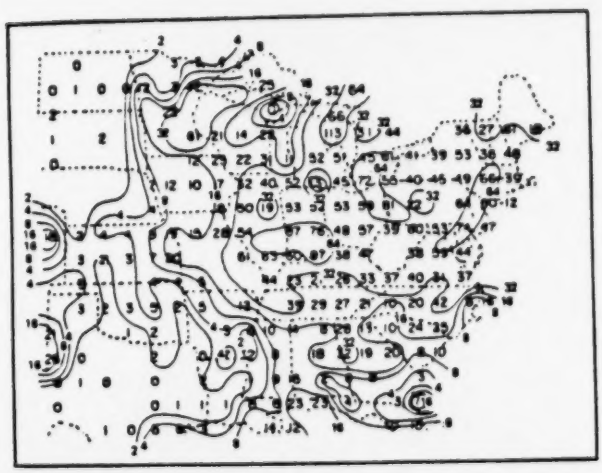

(Lower)

FIGURE 7 CALCULATED (UPPER) AND OBSERVED (LOWER) AIRBORNE SO_2 CONCENTRATIONS ($\mu g\ m^{-3}$) FOR JANUARY 1977.

(Upper)

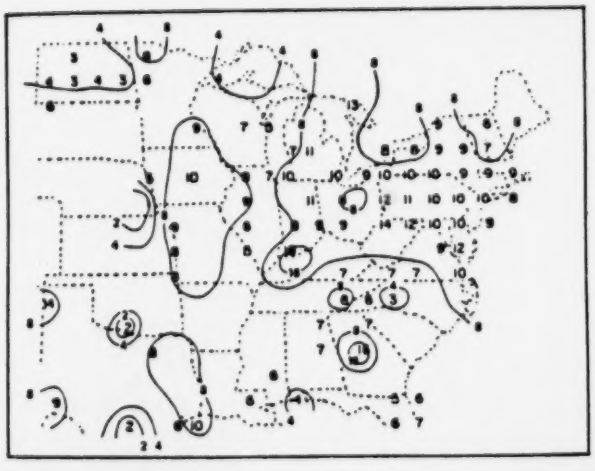

(Lower)

FIGURE 8 CALCULATED (UPPER) AND OBSERVED (LOWER) AIRBORNE $SO_4^=$ CONCENTRATIONS ($\mu g\ m^{-3}$).

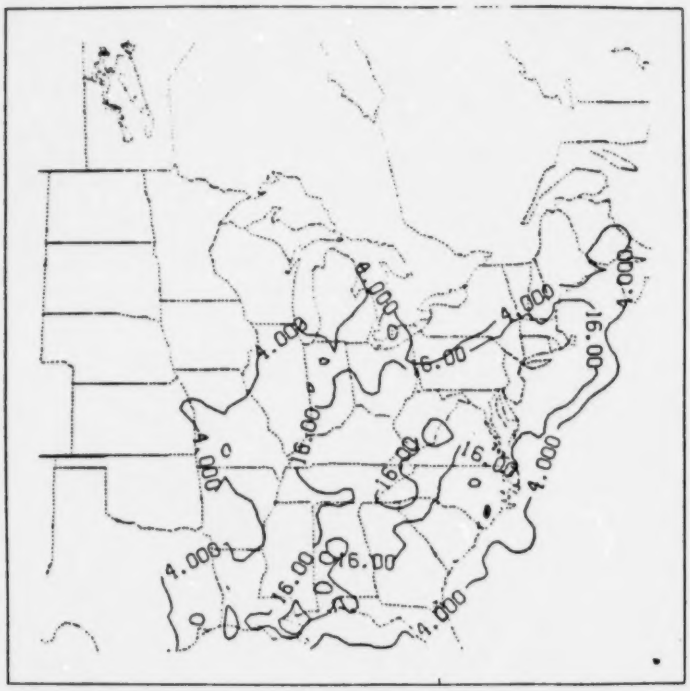

(Upper)

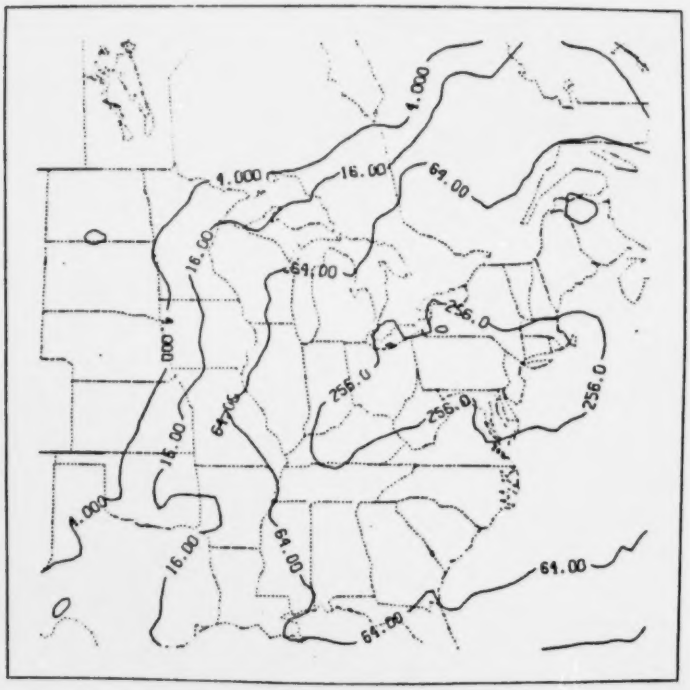

(Lower)

FIGURE 9 CALCULATED WET DEPOSITION (UPPER) AND DRY DEPOSITION (LOWER) OF SO_2 (mg m^{-2}).

(Upper)

(Lower)

FIGURE 10 CALCULATED WET DEPOSITION (UPPER) AND DRY DEPOSITION (LOWER) OF $SO_4^=$ (mg m^{-2}).

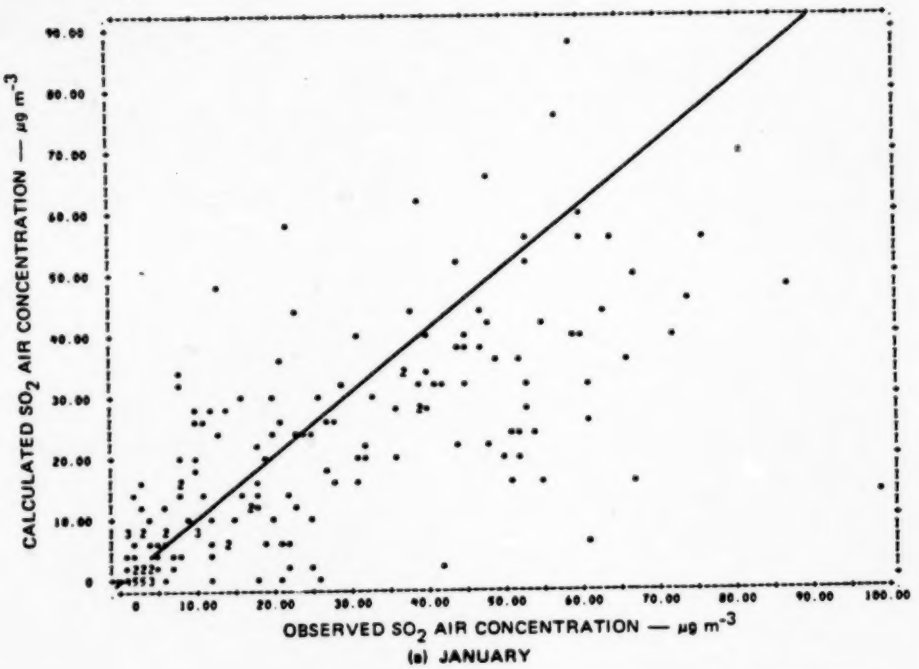

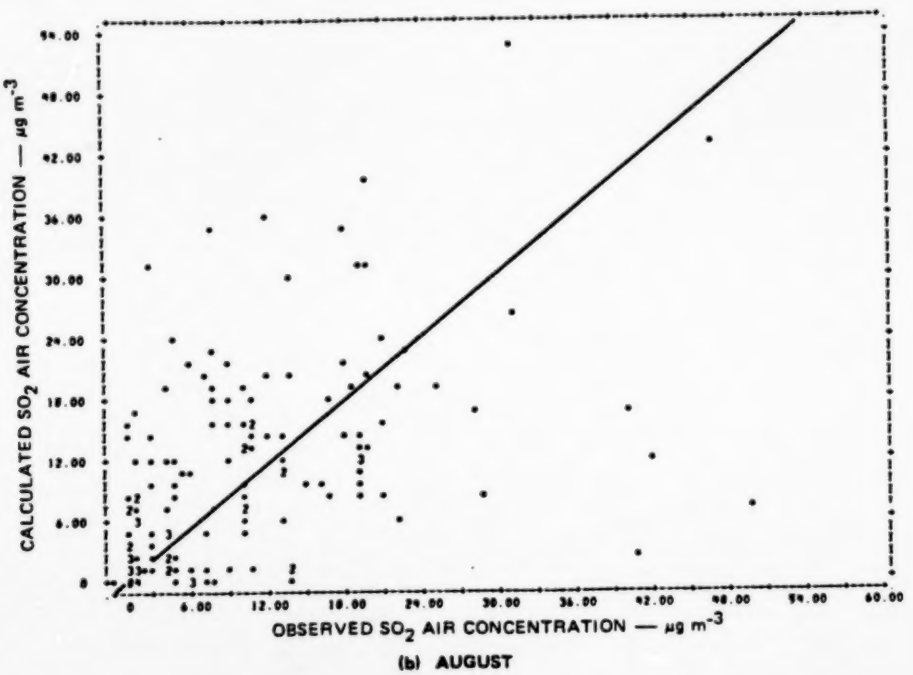

FIGURE 11 SCATTER DIAGRAMS OF OBSERVED MONTHLY VALUES VERSUS CALCULATED VALUES OF SO_2 CONCENTRATIONS FOR JANUARY AND AUGUST 1977.

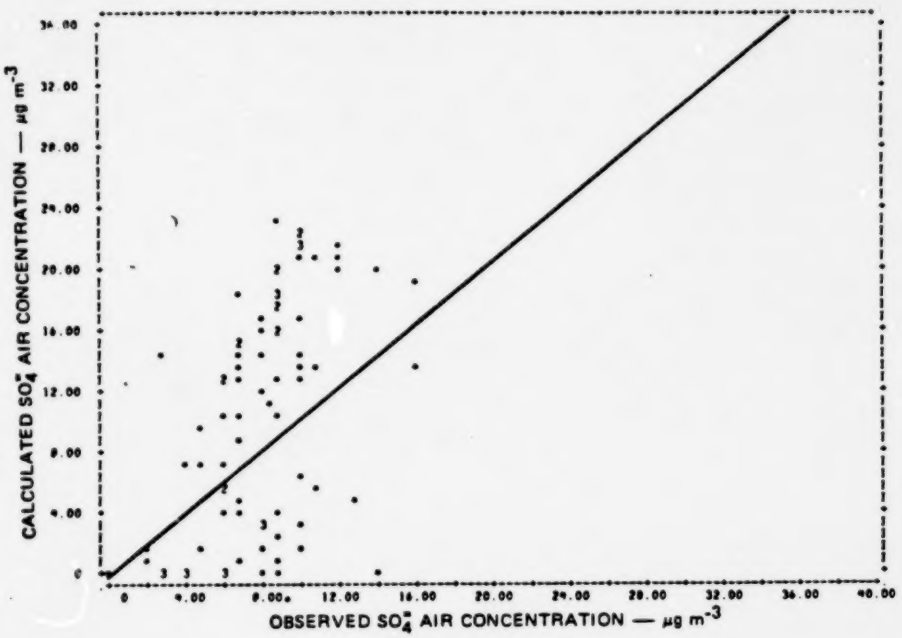

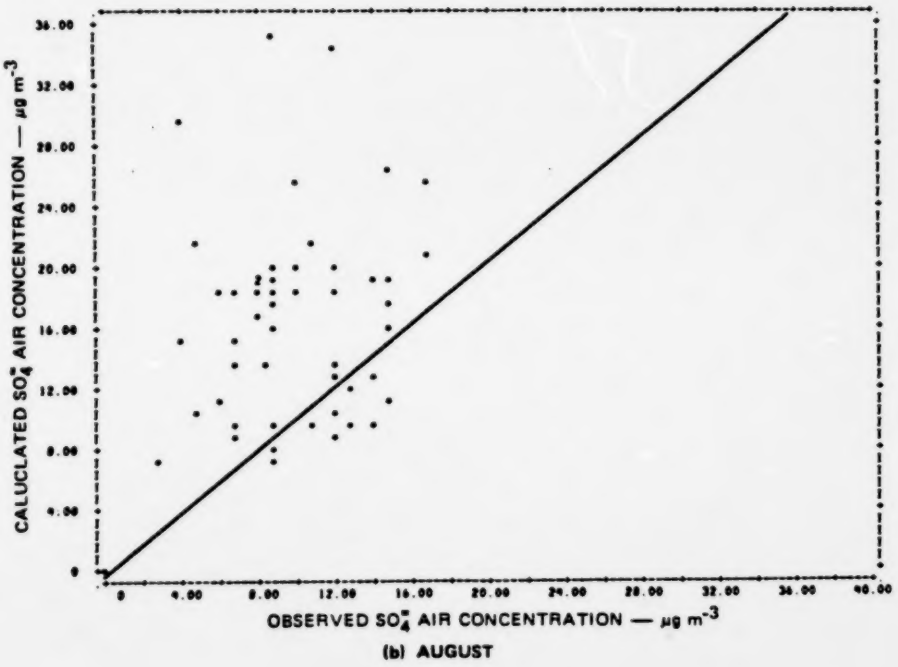

FIGURE 12 SCATTER DIAGRAM OF OBSERVED MONTHLY VALUES VERSUS CALCULATED VALUES OF $SO_4^=$ CONCENTRATIONS FOR JANUARY AND AUGUST 1977.